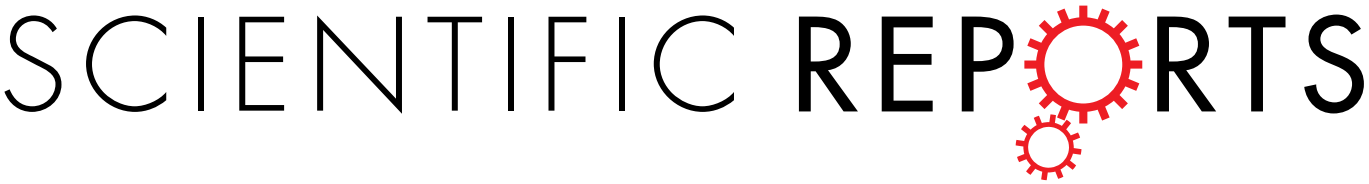

OPEN

Received: 17 November 2015
Accepted: 12 April 2016
Published: 04 May 2016

Novel chemical synthesis and characterization of copper pyrovanadate nanoparticles and its influence on the flame retardancy of polymeric nanocomposites

Maryam Ghiyasiyan-Arani[1], Maryam Masjedi-Arani[2], Davood Ghanbari[2], Samira Bagheri[3] & Masoud Salavati-Niasari[1]

In this work, copper pyrovanadate ($Cu_3V_2O_7(OH)_2(H_2O)_2$) nanoparticles have been synthesized by a simple and rapid chemical precipitation method. Different copper-organic complexes were used to control the size and morphology of products. The morphology and structure of the as-synthesized products were characterized by X-ray diffraction (XRD), scanning electron microscopy (SEM), transmission electron microscopy (TEM), Fourier transform infrared (FT-IR) spectrum, electron dispersive X-ray spectroscopy (EDX), thermal gravimetric analysis (TGA), differential thermal analysis (DTA) and photoluminescence (PL) spectroscopy. The influence of copper pyrovanadate nanostructures on the flame retardancy of the polystyrene, poly vinyl alcohol and cellulose acetate was studied. Dispersed nanoparticles play the role of a magnetic barrier layer, which slows down product volatilization and prevents the flame and oxygen from the sample during decomposition of the polymer. $Cu_3V_2O_7(OH)_2(H_2O)_2$ is converted to $Cu_3V_2O_8$ with an endothermic reaction which simultaneously releases water and decrease the temperature of the flame region.

Considerable attention has been paid to the synthesis of the nanostructured materials during the last decade because of their extensive properties and wide range of applications[1,2]. Nanostructured copper vanadates are widely used in applications such as lithium ion batteries[3–7], antibacterial additive[8], Ion-exchange materials[9], electrochemical properties[10–12] and catalyst[13,14]. There are different types of mixed oxides based on vanadium and copper such as (CuV_2O_6)[15,16], ($Cu_2V_2O_7$)[17,18], ($Cu_3V_2O_8$)[19,20], ($Cu_5V_2O_{10}$)[21] and $Cu_3(OH)_2V_2O_7{\cdot}nH_2O$[7,22]. Volborthite, $Cu_3V_2O_7(OH)_2(H_2O)_2$, is an interesting layered crystalline material that consists of a copper layer, in octahedral coordination with oxygen, joined by vanadium tetrahedral in a coordinated layer. Various methods for the synthesis of copper vanadate have been studied such as laser ablation[23], hydrothermal[12,22], sol-gel[24] and co-precipitation[10]. Precipitation method was used for preparation of $Cu_3V_2O_7(OH)_2(H_2O)_2$ (CVO) nanostructures. The precipitation method is a simple, fast and cost effective synthetic procedure for preparing of copper pyrovanadate nanostructures. To optimize the size, morphology and also properties of $Cu_3V_2O_7(OH)_2(H_2O)_2$ nanostructures, copper-organic complexes ($[Cu(en)_2]SO_4$, $[Cu(pn)_2]SO_4$, [Cu(TETA)]SO_4 and [Cu(TEPA)]SO_4) were chosen as Cu precursor. It has been demonstrated that these kinds of metal-organic complexes have an effective role on size controlling, morphology of the final products[25]. Herein, we report a simple and surfactant-free route for the synthesis of copper pyrovanadate nanostructures via the chemical precipitation method from 3:2 molar ratio of copper-organic complexes and NH_4VO_3. Polymeric nanocomposites have recently gained much attention because adding a small amount of nanostructure to a polymeric matrix can lead to improvement properties of the matrix[26–29]. The principal profits of these compounds over many metallic alloys are corrosion

[1]Institute of Nano Science and Nano Technology, University of Kashan, Kashan, P. O. Box.87317-51167, I. R. Iran. [2]Young Researchers and Elite Club, Arak Branch, Islamic Azad University, Arak, Iran. [3]Nanotechnology & Catalysis Research Centre (NANOCAT), IPS Building, University of. Malaya, 50603 Kuala Lumpur, Malaysia. Correspondence and requests for materials should be addressed to S.B. (email: samira_bagheri@um.edu.my) or M.S.-N. (email: salavati@kashanu.ac.ir)

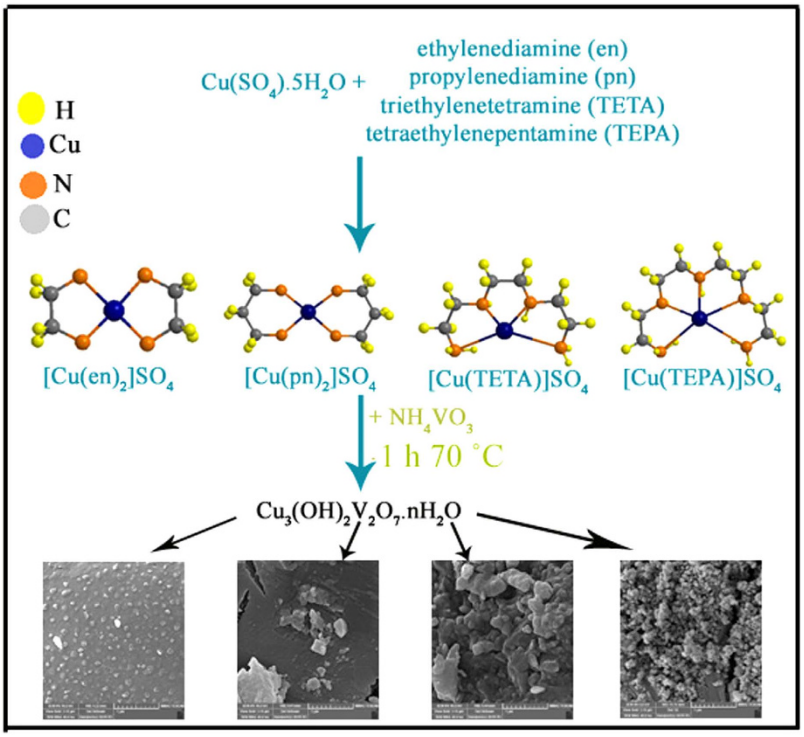

Figure 1. Schematic depiction for the preparation of $Cu_3V_2O_7(OH)_2(H_2O)_2$ nanoparticles.

Sample No.	Cu precursore	Cu:V:amine molar ratio	Particle size (SEM) nm
1	$[Cu(en)_2]SO_4$	3:2:2	50–150
2	$[Cu(pn)_2]SO_4$	3:2:2	Agglomerated particles
3	$[Cu(TETA)]SO_4$	3:2:1	Agglomerated particles
4	$[Cu(TEPA)]SO_4$	3:2:1	10–150

Table 1. Reaction conditions for $Cu_3V_2O_7(OH)_2(H_2O)_2$ nanoparticles.

resistance, low density and thermal insulation. However the main disadvantage of polymeric compounds is high flammability. Using of the most traditional and toxic flame retardants like halogenated and aromatic compounds are forbidden with respect to the environmental considerations. Herein, the influence of copper pyrovanadate nanostructures on the flame retardancy of the polymeric matrix nanocomposites was studied.

Results and Discussion

Figure 1 show schematic diagram of formation of $Cu_3V_2O_7(OH)_2(H_2O)_2$ nanoparticles. The preparation conditions for the synthesis of $Cu_3V_2O_7(OH)_2(H_2O)_2$ nanoparticles have been illustrated in Table 1. Figure 2a shows XRD pattern of copper pyrovanadate sample prepared with copper-organic complex of $[Cu(en)_2]SO_4$ (sample No.1). All diffraction peaks were indexed to pure Monoclinic phase of $Cu_3(OH)_2V_2O_7.nH_2O$ with space group of C2/m and cell constants a = 10.6060 Å, b = 5.8740 Å, and c = 7.2130 Å (JCPDS Card No.80–1169). The crystallite diameter (D_c) of CVO nanostructures has been found to be 45 nm. EDS analysis measurement was employed to investigate the chemical composition and purity of the copper pyrovanadate nanoparticles. EDS analysis of nanoparticles (sample No. 4) is illustrated in Fig. 2b and confirms the presence of Cu, V and O in the sample. According to EDS results, atomic percentage of elements are 4.03% Copper, 15.06% Vanadium and 80.91% Oxygen. Photoluminescence (PL) spectrum of copper pyrovanadate nanoparticles were obtained at room temperature with an excitation wavelength of 375 nm, and is shown in Fig. 2c. The PL spectrum consists of one strong peak at 425 nm. Band gap of as-synthesized sample was obtained to 2.91 eV, which shows blue shift compared with $Cu_3V_2O_7(OH)_2(H_2O)_2$ nanowires (1.94–2.22 eV)[30].

Hysteresis loop and magnetic property of $Cu_3V_2O_7(OH)_2(H_2O)_2$ nanostructures (sample No.4) is shown in Fig. 2d. The saturation magnetization (M_S) and coercivity (Hc) of $Cu_3V_2O_7(OH)_2(H_2O)_2$ nanostructures (sample No.4) are about 0.0117 $emug^{-1}$ and 137 Oe respectively. The behavior of copper pyrovanadate nanoparticles was changed from paramagnetic to ferromagnetic at fields of lower than 1500 Oe. The as-prepared sample shows a twofold behavior, ferromagnetic behavior in low fields and paramagnetic behavior in high fields.

The influence of different copper-organic complexes on the morphology and particle size of copper pyrovanadate samples were investigated by FESEM. Fig. 3a–d show SEM images of copper pyrovanadate samples prepared

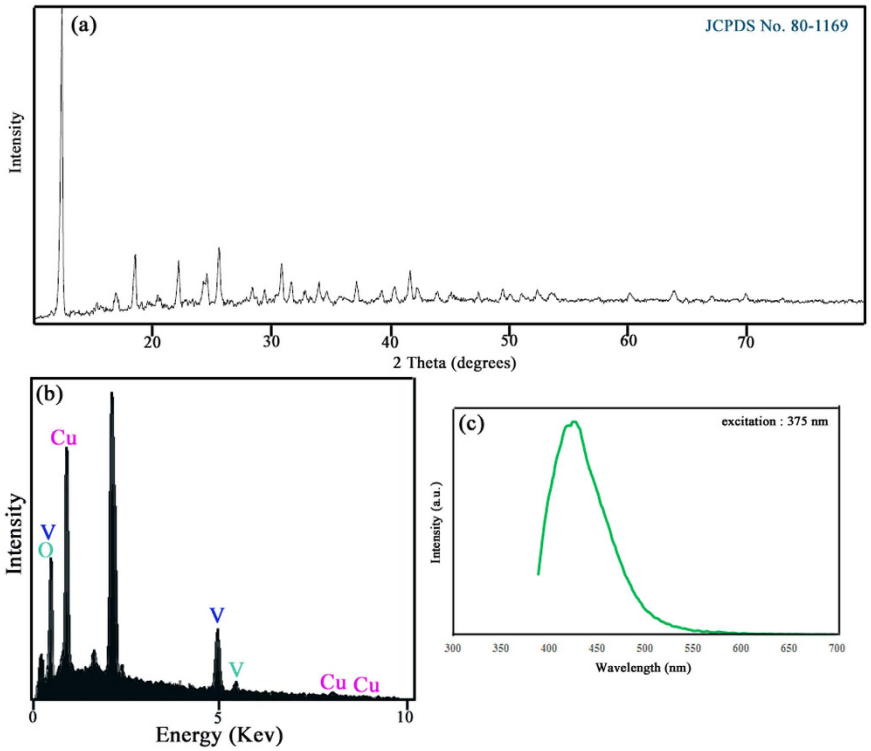

Figure 2. (**a**) XRD, (**b**) EDS patterns, (**c**) Photoluminescence spectrum of pure $Cu_3V_2O_7(OH)_2(H_2O)_2$ nanoparticles (sample No.4) and (**d**) Magnetization versus applied magnetic field at room temperature for the $Cu_3V_2O_7(OH)_2(H_2O)_2$ nanoparticles (sampleNo. 4).

in presence of $[Cu(en)_2]SO_4$, $[Cu(pn)_2]SO_4$, $[Cu(TETA)]SO_4$ and $[Cu(TEPA)]SO_4$ (sample Nos. 1–4) respectively. These results show that using $[Cu(pn)_2]SO_4$ and $[Cu(TETA)]SO_4$ complexes lead to synthesis of agglomerated products. However, by using $[Cu(en)_2]SO_4$ and $[Cu(TEPA)]SO_4$ complexes, nanostructure products are obtained. The particle size of copper pyrovanadate nanostructures obtained with $[Cu(TEPA)]SO_4$ complex are smaller than those produced by $[Cu(en)_2]SO_4$ complex. It is observed that with increasing steric hindrance of complex, a decrease in particle size occurs.

In Fig. 3e, $CuSO_4.5H_2O$ was used as copper source and other reaction parameters remained unchanged. The products obtained from $CuSO_4.5H_2O$ salt as a blank test lead to larger particles than those obtained from Cu-organic complexes. The bulk and agglomerated $Cu_3V_2O_7(OH)_2(H_2O)_2$ products were synthesized by surfactant-free reactions[7,30,31].

The amine ligands in Cu-organic complexes, can act as a capping agent and provide steric hindrance. These results show that using $[Cu(TEPA)]SO_4$ complex lead to synthesis of nano-products. It was observed that with increasing steric hindrance of complex, a decrease in particle size was appeared[32]. Results of particle size of products are shown at Table 1. The precise morphology and particle size of prepared copper pyrovanadate nanostructures with $[Cu(TEPA)]SO_4$ complex was elucidated by TEM. Figure 3f shows the TEM image of sample No. 4 which contains nanoparticles with size of less than 100 nm.

Typical histograms of the particle diameters for the samples obtained using $[Cu(en)_2]SO_4$ and $[Cu(TEPA)]SO_4$ are compared in Fig. 3g, respectively. By comparing the particle size distribution of the products, $Cu_3V_2O_7(OH)_2(H_2O)_2$ that was prepared using $[Cu(TEPA)]SO_4$ have smaller particle size distribution (30–70 nm). By using Cu-organic complexes due to the presence of amine ions in reaction medium, pH of reaction was upper than 6. Whereas, Zhang *et al.* used NH_3 as basic agent in synthesis of $Cu_3V_2O_7(OH)_2(H_2O)_2$ by using $CuSO_4.5H_2O$ and NH_4VO_3 precursors[10]. Moreover, Cu-organic complexes lead to formation of nanostructures and there is no need to use of surfactants. Sun *et al.* used CTAB as a surfactant for preparing of flower-like $Cu_3V_2O_7(OH)_2.2H_2O$ microstructures[31].

Figure 4i(a) shows SEM image of pure poly vinyl alcohol; pure polymers show smooth and flat surfaces and only some cracks due to interaction of polymer and electron beam were observed and also Fig. 4i(b–d) illustrate SEM images PVA-CVO nanocomposite in three different magnifications that obviously confirm presence of spherical nanoparticles in the polymeric nanocomposites. Figure 4ii(a) shows SEM image of flat poly styrene surface and Fig. 4ii(b–d) illustrate SEM images PS-CVO in approve the presence of nanoparticles in the polymeric nanocomposites. Because of hydrophilic property of CVO and hydrophobic of poly styrene there is an expected agglomeration in PS-CVO nanocomposite. Figure 4iii(a) also exhibit SEM image of smooth cellulose acetate Fig. 4iii(b–d) give SEM images of CA-CVO that appropriately show nanoparticles in the polymeric nanocomposites. Figures 5(a–d) show FT-IR spectra of the $[Cu(en)_2]SO_4$, $[Cu(pn)_2]SO_4$, $[Cu(TETA)]SO_4$ and $[Cu(TEPA)]SO_4$ complexes, respectively. In these spectra, the absorption around 3230 cm^{-1} can be assigned to the stretching

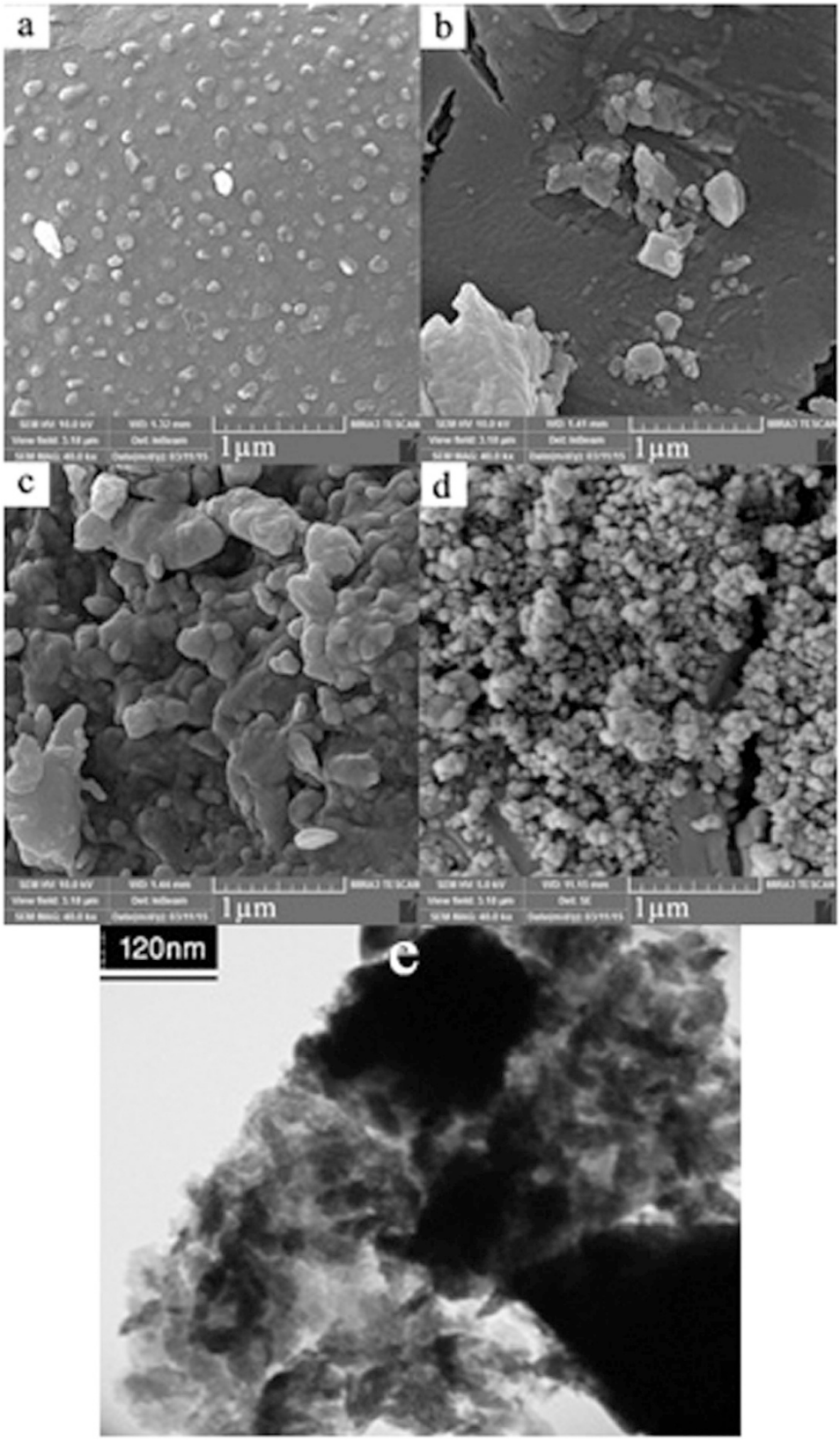

Figure 3. SEM images of the $Cu_3(OH)_2V_2O_7.nH_2O$ nanoparticles with different copper-organic complexes (**a**) $[Cu(en)_2]SO_4$, (**b**) $[Cu(pn)_2]SO_4$, (**c**) $[Cu(TETA)]SO_4$, (**d**) $[Cu(TEPA)]SO_4$, (**e**) $CuSO_4.5H_2O$, f) TEM image of nanostructures obtained with $[Cu(TEPA)]SO_4$ and g) Particle size distribution of samples Nos. 1 and 4.

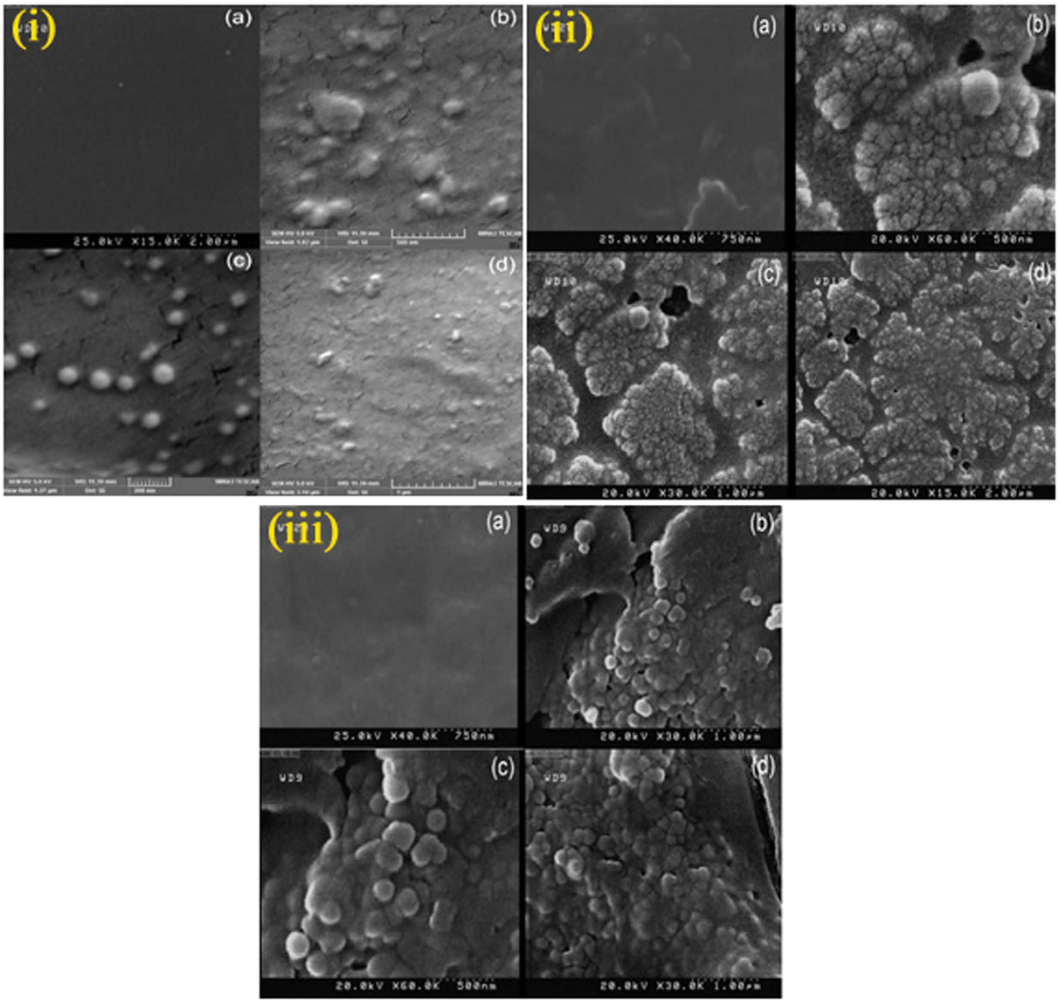

Figure 4. SEM images of the (i): (**a**) pure PVA (b,c,d) PVA nanocomposite, ii: (**a**) pure PS (**b–d**) PS nanocomposite and (iii): (**a**) pure CA (**b–d**) CA nanocomposite.

vibration of the N-H of amine groups. Two absorption bands around 2940 and 2880 cm^{-1} can be assigned to the symmetry stretching and asymmetry stretching mode of the CH_2 groups, respectively. The bands around 3300, 1610, 930 and 620 cm^{-1} can be related to water molecules. The absorption bands at 1440 and 1054 cm^{-1} can be attributed to the C–H bending vibration and C–N stretching vibration, respectively. The bands at 504 and below 480 cm^{-1} is assigned to m(Cu–O) and m(Cu–N) vibration, respectively. FT-IR spectrum of CVO is shown in Fig. 5(e–h) absorptions at 450 and 3249 cm^{-1} are related to Cu-O and O-H bonds respectively. Figure 5f illustrates spectrum of CA–CVO nanocomposite, absorptions at 1083 and 3470 cm^{-1} are attributed to C-O and hydroxyl bonds respectively and peaks at 1440 and 1600 cm^{-1} are responsible to C = O bonds. Spectrum of PS–CVO nanocomposite is depicted in Fig. 5g in which the peak absorptions at 2922 and 3028 cm^{-1} are related to aliphatic and aromatic C–H bonds, respectively. Spectrum of PVA–CVO nanocomposite is depicted in Fig. 5h which the peak at 1090 cm^{-1} is related to V-O bond. Peaks at 1561 and 1747 cm^{-1} are correspond to C = O bonds and also absorptions at 1083 and 3470 cm^{-1} are attributed to C-O[33–35].

The effect of inorganic nanostructure on the flame retardant properties of the polymers has been considered using UL-94 test. The outcomes show that CVO additives can enhance the flame retardant property of the polymeric matrices. *Ex-situ* products were easily obtained and made from two separated phases of copper pyrovanadate and polymeric matrices. The main challenge in the synthesis of nanocomposite is dispersion of inorganic phase in organic matrix. Hydroxyl group in copper pyrovanadate nanoparticles lead to suitable interaction with hydrophilic polymers like vinyl alcohol and cellulose acetate matrices. The results of UL-94 tests for poly styrene and cellulose acetate nanocomposites are NC and V-1 respectively (Fig. 6a–d). The worst result was obtained for PS-CVO because of incompatibility of hydrophobic polystyrene and hydrophilic CVO. The result of UL-94 tests for poly vinyl alcohol nanocomposites is V-0. HO…Cu-V-O-Cu…OH compound and other precursors as binder are compatible with polymeric matrices. The enhancement of flame retardancy of nanocomposite is due to formation of effective barrier layer of Cu-V-O that precludes flame and oxygen reaching to the nanocomposites (Fig. 6e–g).

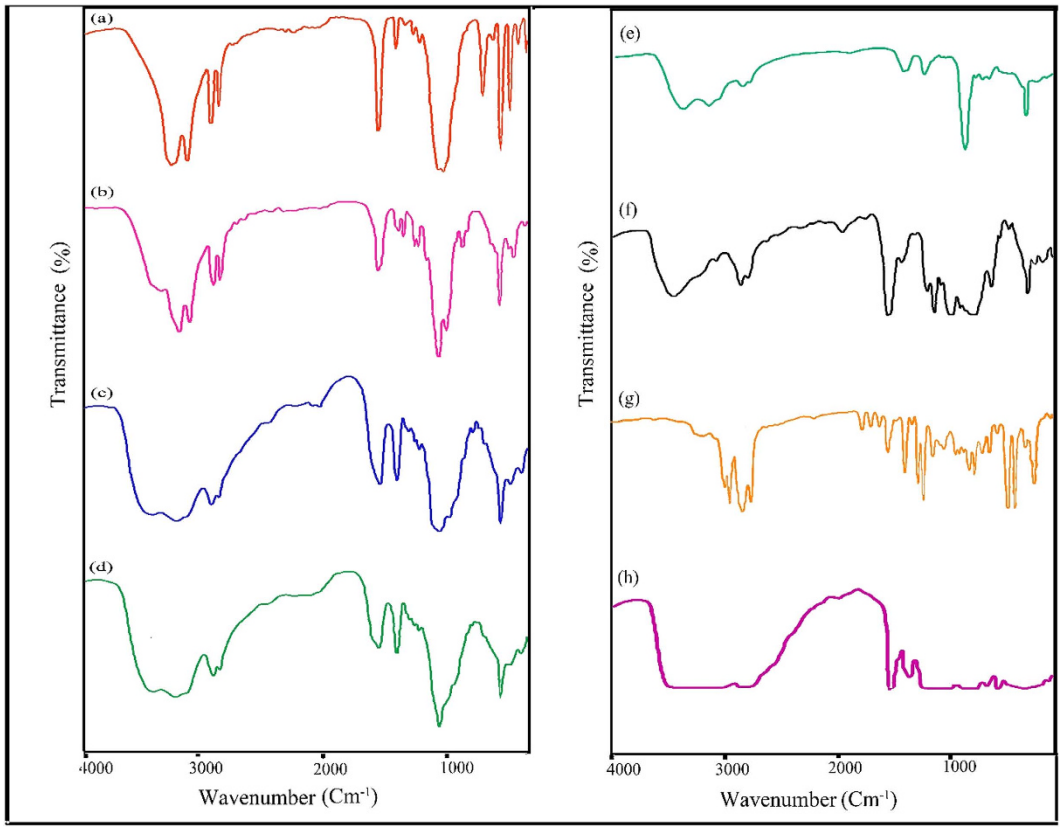

Figure 5. FT-IR spectra of (**a**) $[Cu(en)_2]SO_4$, (**b**) $[Cu(pn)_2]SO_4$, (**c**) [Cu(TETA)]SO_4, (**d**) [Cu(TEPA)]SO_4, (**e**) CVO nanoparticles, (**f**) CA, (**g**) PS and (**h**) PVA.

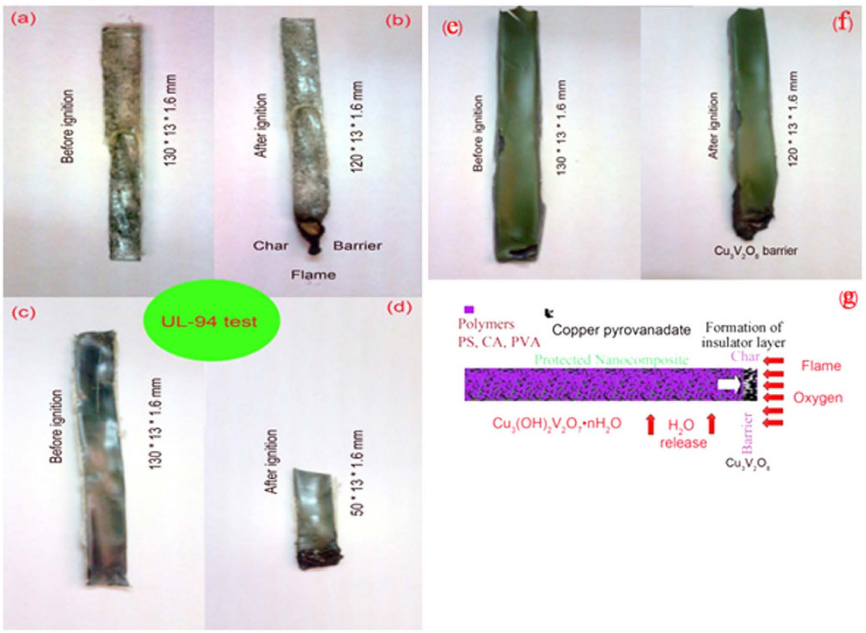

Figure 6. UL 94 analysis of the (**a,b**) CA (**c,d**) PS (**e,f**) PVA (**g**) schematic of barrier formation.

Dispersed nanoparticles play the role of a magnetic barrier layer[22] which slows down product volatilization and prevents flame and oxygen from the sample during decomposition of the polymer. $Cu_3(OH)_2V_2O_7{\cdot}2H_2O$ is converted to $Cu_3V_2O_8$ with an endothermic reaction releases water and decreases temperature of the flame region

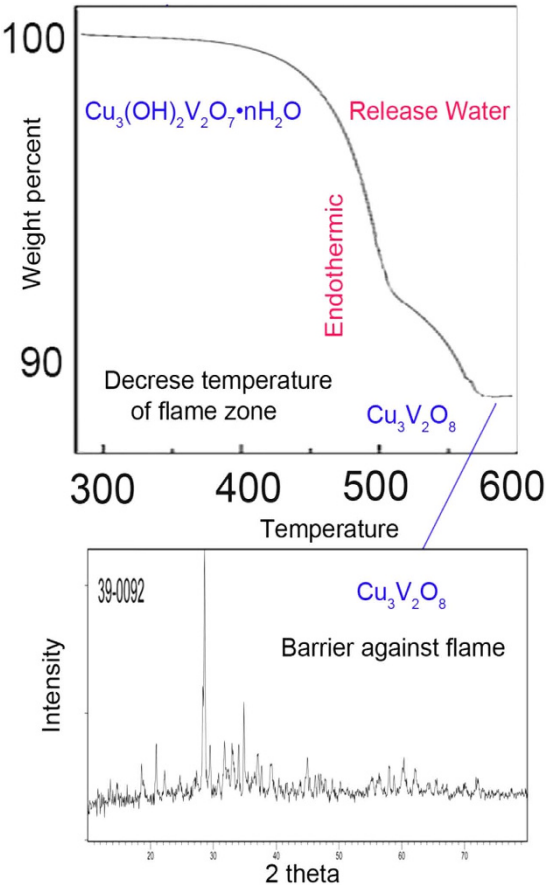

Figure 7. (**a**) TGA of $Cu_3V_2O_7(OH)_2(H_2O)_2$ and (**b**) conversion to $Cu_3V_2O_8$ (**c**) DTA.

(Fig. 7). Water vapour also dilutes flammable gases in the fire zone. In the presence of flame, magnetic nanoparticles remain together (show resistance to drop falling) and build a barrier.

$Cu_3V_2O_7(OH)_2(H_2O)_2$ is a hydrophilic product that show the best dispersion in water and as a results approve the best compatibility with hydrophilic PVA. Acetone as the second solvent for dispersing nanoparticles and dichloromethane has the worst compatibility with hydroxyls of the nanoparticles and as shown in SEM images agglomerated nanoparticles in the poly styrene matrix was observed.

Molar mass of $Cu_3V_2O_7(OH)_2(H_2O)_2$ is 474.5 g, at the first decomposition, $2H_2O$ were evaporated from compound (36 g/474.5 g = 8%). At the second step of decomposition, another OH_2 was evaporated (18 g/474 g.5 = 4%). The experimental results that were achieved from TGA analysis (8% weight loss at 450 °C and 4% weight loss at 550 °C = totally 12%) have suitable agreement with theoretical results for preparation of $Cu_3V_2O_8$ (420.5 g/474.5 g = 88%) as a residual compound (Fig. 7b). Endothermic reaction was investigated and was confirmed by differential thermal analysis (DTA) and is shown in Fig. 7c. The flame retardancy could be a source of the char consisting of mainly $Cu_3V_2O_8$ just blocking the air from reacting with the polymer. Actually flame retardancy in this work is result of synergism of barrier effect of nanostructure, release of water ($3H_2O$: cooling the flame region) and endothermic decomposition (absorption the heating of flame zone)[36]. Also because of magnetic property of the nanostructures a compact and dense barrier is produced.

Experimental

Materials and Physical Measurements. $CuSO_4.5H_2O$, NH_4VO_3, ethylenediamine (en), propylenediamine (pn), triethylenetetramine (TETA) and tetraethylenepentamine (TEPA) were purchased from Merck Company. All of the chemicals were used as received without further purifications. For characterization of the products, X-ray diffraction (XRD) patterns were recorded by a Rigaku D-max C III, X-ray diffractometer using Ni-filtered Cu Ka radiation. Scanning electron microscopy (SEM) images were obtained on Philips XL-30ESEM. Transmission electron microscopy (TEM) image was obtained on a Philips EM208 transmission electron microscope with an accelerating voltage of 200 kV. Fourier transform infrared (FT-IR) spectra were recorded on Shimadzu Varian 4300 spectrophotometer in KBr pellets. The magnetic properties of the samples were detected at room temperature using a vibrating sample magnetometer (VSM, Meghnatis Kavir Kashan Co., Kashan, Iran). Room temperature photoluminescence (PL) was studied on a Perkin Elmer (LS 55) fluorescence spectrophotometer.

Synthesis of Cu-organic complexes. An aqueous solution including 1 mol of $CuSO_4.5H_2O$ in 50 mL of distilled water was added to a stoichiometric amount of ethylenediamine in 50 mL of distilled water under magnetic stirring. The mixture was stirred and heated (80 °C) for 5 h. The blue obtained precipitate was centrifuged, washed with ethanol and distilled water and dried at 50 °C. Other complexes were prepared via mentioned method.

Synthesis of pure $Cu_3V2O_7(OH)_2(H2O)_2$ nanoparticles. First, 0.5 g of Cu-organic complex was dissolved into deionized water and was added to aqueous solution of NH_4VO_3 with a molar ratio of Cu:V = 3:2. After that, the above solution was heated at 100 °C and stirred for 1–2 h. The black precipitate was dried at 80 °C under vacuum for 2 h. In Scheme. 1, schematic diagram of formation of $Cu_3V_2O_7(OH)_2(H_2O)_2$ nanoparticles is depicted. The preparation conditions for synthesis $Cu_3V_2O_7(OH)_2(H_2O)_2$ nanoparticles have been illustrated in Table 1.

Preparation of *ex-situ* nanocomposites. 5 g of polymer was dissolved in 10 mL of solvent (25 °C) and then $Cu_3V_2O_7(OH)_2(H_2O)_2$ nanoparticles (1 g) was dispersed in 5 mL of solvent with ultrasonic waves (20 min, 60 W). Next, the dispersion of copper pyrovanadate was added slowly to the polymer solution. Solvent for poly styrene (PS), poly vinyl alcohol(PVA) and cellulose acetate (CA) are dichloromethane, water and acetone respectively. The solution was mixed under stirring for 6 h. For preparation of samples for UL-94 test after stirring, the product was casted on a template with dimension 130 × 13 mm and after about 48 h of solvent evaporation; the nanocomposite was placed in the vacuum oven for another 5 h for removal of residual traces of solvent. The final sheets for the test are 130 × 13 × 1.6 mm in dimension.

In UL-94 test a bar shape specimen of plastic 130 × 13 × 1.6 mm is positioned vertically and held from the top. A Bunsen burner flame is applied to the specimen twice (10 s each). A V-0 classification is given to material that is extinguished in less than 10 s after any flame application, drips of particles allowed as long as they are not inflamed. A V-1 classification is received by a sample with maximum combustion time <30 s, drips of particles allowed as long as they are not inflamed. The sample is classified V-2 if it satisfies the combustion time criteria of V-1, but flaming drips are allowed. Materials are ranked as N.C. in UL-94 tests when the maximum total flaming time is above 50 s. The sample is classified HB when slow burning on a horizontal specimen; burning rate <76 mm/min [28, 29].

References

1. Masjedi-Arani, M., Salavati-Niasari, M., Ghanbari, D. & Nabiyouni, G. A sonochemical-assisted synthesis of spherical silica nanostructures by using a new capping agent. *Ceram. Int.* **40,** 495–499 (2014).
2. Masjedi, M. *et al.* Effect of Schiff base ligand on the size and the optical properties of TiO_2 nanoparticles. *Superlattices Microstruct*. **62,** 30–38 (2013).
3. Choi, J.-H. *et al.* Multi-layer electrode with nano-$Li_4Ti_5O_{12}$ aggregates sandwiched between carbon nanotube and graphene networks for high power Li-ion batteries. *Sci. rep*. **4,** 7334; 10.1038/srep07334 (2014).
4. Dai, B., Wang, Q., Yu, F. & Zhu, M. Effect of Au nano-particle aggregation on the deactivation of the $AuCl_3$/AC catalyst for acetylene hydrochlorination. *Sci. rep*. **5,** 10553; 10.1038/srep10553 (2015).
5. Bhadra, C. M. *et al.* Antibacterial titanium nano-patterned arrays inspired by dragonfly wings. *Sci. rep*. **5,** 16817, doi: 10.1038/srep16817 (2015).
6. Cao, X., Xie, J., Zhan, H. & Zhou, Y. Synthesis of CuV 2 O 6 as a cathode material for rechargeable lithium batteries from V_2O_5 gel. *Mater. Chem. Phys.* **98,** 71–75 (2006).
7. Ni, S., He, D., Yang, X. & Li, T. Hydrothermal synthesis of $Cu_3(OH)_2V_2O_7 \cdot nH_2O$ nanoparticles and its application in lithium ion battery. *J. Alloys Compd.* **509,** L142–L144 (2011).
8. Holtz, R. D. *et al.* Nanostructured silver vanadate as a promising antibacterial additive to water-based paints. *Nanomed: Nanotech, Biolo Med*. **8,** 935–940 (2012).
9. El-Latif, M. A. & Elkady, M. Synthesis, characterization and evaluation of nano-zirconium vanadate ion exchanger by using three different preparation techniques. *Mater. Res. Bull.* **46,** 105–118 (2011).
10. Zhang, S., Ci, L. & Liu, H. Synthesis, characterization, and electrochemical properties of $Cu_3V_2O_7(OH)_2 \cdot 2H_2O$ nanostructures. *J. Phys. Chem. C.* **113,** 8624–8629 (2009).
11. Zhang, S., Sun, Y., Li, C. & Hu, R. Rational synthesis of copper vanadates/polypyrrole nanowires with enhanced electrochemical property. *Mater. Lett.* **91,** 154–157 (2013).
12. Sun, X. *et al.* Hydrothermal synthesis of $Cu_3V_2O_7(OH)_2 \cdot 2H_2O$ hierarchical microspheres and their electrochemical properties. *Mater. Lett.* **64,** 2019–2021 (2010).
13. Palacio, L. *et al.* Performance of supported catalysts based on a new copper vanadate-type precursor for catalytic oxidation of toluene. *J. Hazard. Mater.* **153,** 628–634 (2008).
14. Palacio, L. A., Silva, J. M., Ribeiro, F. R. & Ribeiro, M. F. Catalytic oxidation of volatile organic compounds with a new precursor type copper vanadate. *Catal. Today.* **133,** 502–508 (2008).
15. Wei, Y. *et al.* Synthesis and structural properties of stoichiometric and oxygen deficient CuV_2O_6 prepared via co-precipitation method. *Solid State Ionics*. **176,** 2243–2249 (2005).
16. Cao, J.-q. *et al.* Sol–gel synthesis and electrochemical properties of CuV_2O_6 cathode material. *J. Alloys Compd.* **479,** 875–878 (2009).
17. Sivakumar, V. *et al.* Copper vanadate nanoparticles: synthesis, characterization and its electrochemical sensing property. *J Mater Sci: Mater Electron*. **25,** 1485–1491 (2014).
18. Ponomarenko, L., Vasil'ev, A., Antipov, E. & Velikodny, Y. A. Magnetic properties of $Cu_2V_2O_7$. *Physica B: Condensed Matter*. **284,** 1459–1460 (2000).
19. Seabold, J. A. & Neale, N. R. All First Row Transition Metal Oxide Photoanode for Water Splitting Based on $Cu_3V_2O_8$. *Chem. Mater.* **27,** 1005–1013 (2015).
20. Zhang, S., Sun, Y., Li, C. & Ci, L. $Cu_3V_2O_8$ hollow spheres in photocatalysis and primary lithium batteries. *Solid-State Sci.* **25,** 15–21 (2013).
21. Dai, J., LaFollette, R. M. & Reisner, D. Thin Film $Cu_5V_2O_{10}$ Electrode for Thermal Batteries. *Meeting Abstracts: J. Electrochem. Soc.* 346–346 (2010).
22. Ni, S. *et al.* Hydrothermal synthesis and magnetic property of $Cu_3(OH)_2V_2O_7 \cdot nH_2O$. *Mater. Lett.* **64,** 516–519 (2010).
23. Liang, Y., Liu, P., Li, H. & Yang, G. Synthesis and characterization of copper vanadate nanostructures via electrochemistry assisted laser ablation in liquid and the optical multi-absorptions performance. *Cryst. Eng. Comm*. **14,** 3291–3296 (2012).

24. Melghit, K. & Wen, L. S. The effect of starting materials on the morphology and particle size of copper pyrovanadate $Cu_3V_2O_7(OH)_2{\cdot}2H_2O$. *Ceram. Int*. **31,** 223–225 (2005).
25. Masjedi-Arani, M. & Salavati-Niasari, M. A simple solid-state approach for synthesis and characterization of $CdO–ZrO_2–CdZrO_3$ nanocomposites. *J Mater Sci: Mater Electron*. **26,** 2316–2322 (2015).
26. Esmaeili-Bafghi-Karimabad, A. *et al.* Photo-catalyst tin dioxide: synthesis and characterization different morphologies of SnO2 nanostructures and nanocomposites. *J Mater Sci: Mater Electron.* **26,** 6970–6978 (2015).
27. Saffari, J. *et al.* Sonochemical synthesis of Fe_3O_4/ZnO magnetic nanocomposites and their application in photo-catalytic degradation of various organic dyes. *J Mater Sci: Mater Electron*. **26,** 9591–9599 (2015).
28. Ghanbari, D., Salavati-Niasari, M. & Ghasemi-Kooch, M. A sonochemical method for synthesis of Fe_3O_4 nanoparticles and thermal stable PVA-based magnetic nanocomposite. *J.Ind. Eng. Chem.* **20,** 3970–3974 (2014).
29. Jamshidi, P., Ghanbari, D. & Salavati-Niasari, M. Sonochemical synthesis of $La(OH)_3$ nanoparticle and its influence on the flame retardancy of cellulose acetate nanocomposite. *J.Ind. Eng. Chem.* **20,** 3507–3512 (2014).
30. Zhang, S. & Ci, L. Synthesis and formation mechanism of $Cu_3V_2O_7(OH)_2{\cdot}\ 2H_2O$ nanowires. *Mater. Res. Bull.* **44,** 2027–2032 (2009).
31. Sun, X. *et al.* Surfactant-assisted hydrothermal synthesis and electrochemical properties of nanoplate-assembled 3D flower-like $Cu_3V_2O_7(OH)_2{\cdot}2H_2O$ microstructures. *Cryst. Eng. Comm*. **13,** 367–370 (2011).
32. Motahari, F., Mozdianfard, M.-R., Soofivand, F. & Salavati-Niasari, M. Binary Roles of Schiff Bases as Capping Agent and Precursor for Synthesis of Metallic *Nickel Ultrafine Nanoparticles. Synth React Inorg Met Org Chem*. **45,** 1449–1456 (2015).
33. Salavati-Niasari, M. & Ghanbari, D. Hydrothermal synthesis of star-like and dendritic PbS nanoparticles from new precursors. *Particuology.* **10,** 628– 633 (2012).
34. Salavati-Niasari, M., Ghanbari, D. & Davar, F. Synthesis of Different Morphologies of PbS Nanostructures via Hydrothermal Process. *High Temp. Mater. Proc*. **31,** 707–710 (2012).
35. Esmaeili-Zare, M., Salavati-Niasari, M., Ghanbari, D. & Aminifazl, A. A Facile Sonochemical Method for Synthesis of Mercury Selenide Nanostructures. *J Clust Sci.* **24,** 881–890 (2013).
36. Ghanbari, D., Salavati-Niasari, M. & Sabet, M. Preparation of flower-like magnesium hydroxide nanostructure and its influence on the thermal stability of poly vinyl acetate and poly vinyl alcohol. *Composites B: Eng* **45,** 550–555 (2013).

Acknowledgements

This work is financially supported by University Malaya Research Grant (RP038B-15HTM) and the council of University of Kashan by Grant No (159271/779).

Author Contributions

M.S.N., M.M.A., D.G. and M.G.A. conceived the idea. M.G.A. conducted the experiments, S.B. and M.S.N. helped for characterization of products. M.M.A. and D.G. wrote the manuscript. All authors reviewed the manuscript.

Additional Information

Competing financial interests: The authors declare no competing financial interests.

How to cite this article: Ghiyasiyan-Arani, M. *et al.* Novel chemical synthesis and characterization of copper pyrovanadate nanoparticles and its influence on the flame retardancy of polymeric nanocomposites. *Sci. Rep.* **6**, 25231; doi: 10.1038/srep25231 (2016).